doi:10.1093/brain/awr199 Brain 2011: 134; 2736–2754 | 2736

BRAIN
A JOURNAL OF NEUROLOGY

Inhibition of soluble tumour necrosis factor is therapeutic in experimental autoimmune encephalomyelitis and promotes axon preservation and remyelination

Roberta Brambilla,[1] Jessica Jopek Ashbaugh,[1,2] Roberta Magliozzi,[3] Anna Dellarole,[1] Shaffiat Karmally,[1] David E. Szymkowski[4] and John R. Bethea[1,2,5]

1 The Miami Project To Cure Paralysis, Miller School of Medicine, University of Miami, 1095 NW 14th Terrace, Miami, FL 33136, USA
2 Department of Microbiology and Immunology, Miller School of Medicine, University of Miami, Miami, FL 33136, USA
3 Department of Cell Biology and Neuroscience, Istituto Superiore di Sanità, 00161 Rome, Italy
4 Xencor Inc., 111 West Lemon Avenue, Monrovia, CA 91016, USA
5 The Neuroscience Program, Miller School of Medicine, University of Miami, Miami, FL 33136, USA

Correspondence to: Roberta Brambilla, PhD,
The Miami Project To Cure Paralysis,
Miller School of Medicine, University of Miami
1095 NW 14th Terrace,
Miami, FL 33136, USA.
E-mail: r.brambilla@miami.edu

Correspondence may also be addressed to: John R. Bethea. E-mail: jbethea@miami.edu

Tumour necrosis factor is linked to the pathophysiology of various neurodegenerative disorders including multiple sclerosis. Tumour necrosis factor exists in two biologically active forms, soluble and transmembrane. Here we show that selective inhibition of soluble tumour necrosis factor is therapeutic in experimental autoimmune encephalomyelitis. Treatment with XPro1595, a selective soluble tumour necrosis factor blocker, improves the clinical outcome, whereas non-selective inhibition of both forms of tumour necrosis factor with etanercept does not result in protection. The therapeutic effect of XPro1595 is associated with axon preservation and improved myelin compaction, paralleled by increased expression of axon-specific molecules (e.g. neurofilament-H) and reduced expression of non-phosphorylated neurofilament-H which is associated with axon damage. XPro1595-treated mice show significant remyelination accompanied by elevated expression of myelin-specific genes and increased numbers of oligodendrocyte precursors. Immunohistochemical characterization of tumour necrosis factor receptors in the spinal cord following experimental autoimmune encephalomyelitis shows tumour necrosis factor receptor 1 expression in neurons, oligodendrocytes and astrocytes, while tumour necrosis factor receptor 2 is localized in oligodendrocytes, oligodendrocyte precursors, astrocytes and macrophages/microglia. Importantly, a similar pattern of expression is found in post-mortem spinal cord of patients affected by progressive multiple sclerosis, suggesting that pharmacological modulation of tumour necrosis factor receptor signalling may represent an important target in affecting not only the course of mouse experimental autoimmune encephalomyelitis but human multiple sclerosis as well. Collectively, our data demonstrate that selective inhibition of soluble tumour necrosis factor improves recovery following experimental autoimmune encephalomyelitis, and that signalling mediated by transmembrane tumour necrosis factor is essential for axon and myelin preservation as well as remyelination, opening the possibility of a new avenue of treatment for multiple sclerosis.

Received May 11, 2011. Revised July 1, 2011. Accepted July 9, 2011

Keywords: demyelination; multiple sclerosis; neurodegenerative disorders; neuroprotection; myelin repair

Abbreviations: EAE = experimental autoimmune encephalomyelitis; MOG = myelin oligodendrocyte glycoprotein; TNF = tumour necrosis factor

Introduction

Tumour necrosis factor (TNF) is a pleiotropic cytokine involved in the regulation of numerous physiological and pathological processes, such as inflammation, cancer, autoimmunity and infection. TNF exists in two biologically active forms, transmembrane TNF and soluble TNF. The cellular functions of TNF are mediated by TNF receptor 1 (TNFR1) and TNF receptor 2 (TNFR2), which differ in expression profiles, ligand affinity, cytoplasmic tail structure and downstream signalling pathway activation. TNFR1, unlike TNFR2, contains a death domain (DD) localized within the cytoplasmic segment. Soluble TNF and transmembrane TNF are capable of binding to both receptors, although with significantly different binding affinities. As a consequence, soluble TNF, which has higher affinity for TNFR1, primarily signals through TNFR1, mediating apoptosis and chronic inflammation (Holtmann and Neurath, 2004). Conversely transmembrane TNF, with higher affinity for TNFR2, preferentially signals through this receptor (Grell *et al*., 1995; Wajant *et al*., 2003), regulating gene programs important for cell survival, resolution of inflammation, maintenance of immunity to pathogens and myelination (Pasparakis *et al*., 1996; Arnett *et al*., 2001; Canault *et al*., 2004; Olleros *et al*., 2005, 2009; Alexopoulou *et al*., 2006; Ierna *et al*., 2009). It is therefore apparent that the two forms of TNF have specific and often opposing biological effects, which may explain the contrasting outcomes of TNF inhibition both in animal models of demyelinating diseases and human clinical trials. Indeed, non-selective anti-TNF biologics (e.g. infliximab, adalimumab, etanercept, certolizumab pegol and golimumab) are successfully used in treating TNF-mediated pathologies such as rheumatoid arthritis, psoriatic arthritis and Crohn's disease (Tracey *et al*., 2008); however, they are associated with serious adverse effects such as congestive heart failure, increased risk of infection and demyelination (Ramos-Casals *et al*., 2008; Fromont *et al*., 2009; Wallis, 2009; Sfikakis, 2010).

TNF is also linked to the development of various neurological/neurodegenerative disorders, including multiple sclerosis (McCoy and Tansey, 2008). Patients with multiple sclerosis manifest elevated concentrations of TNF in serum, CSF (Maimone *et al*., 1991; Sharief and Hentges, 1991; Spuler *et al*., 1996) and within active lesions (Hofman *et al*., 1989; Selmaj *et al*., 1991). Peaks of serum and CSF TNF are correlated with the presence of active MRI-detectable multiple sclerosis lesions (Spuler *et al*., 1996). Furthermore, overexpression of TNF in mice leads to demyelinating disease (Probert *et al*., 1995; Akassoglou *et al*., 1998; Dal Canto *et al*., 1999) and in animal models of multiple sclerosis, e.g. experimental autoimmune encephalomyelitis (EAE), TNF blockade prevents or ameliorates the pathology (Ruddle *et al*., 1990; Baker *et al*., 1994).

Such compelling evidence in human disease and animal models led, in 1997, to the first multiple sclerosis clinical trial with a non-selective TNF inhibitor, lenercept. Against all expectations, the trial had to be abruptly terminated due to dose-dependent increases in frequency, duration and severity of multiple sclerosis attacks (Lenercept-Group, 1999). The failure of the trial underscored the necessity for more in-depth studies to better understand the complex roles of TNF in multiple sclerosis pathology. Studies in animal models of multiple sclerosis showed that the absence of TNF or TNFR1/TNFR2 combined does not protect from the pathology, only delays it and induces exacerbation of chronic disease (Korner *et al*., 1997; Liu *et al*., 1998; Eugster *et al*., 1999; Kassiotis *et al*., 1999; Suvannavejh *et al*., 2000). TNFR1$^{-/-}$ mice, which lack the receptor preferentially activated by soluble TNF, are protected from EAE, show faster regression of the pathology and remyelinate normally (Eugster *et al*., 1999; Suvannavejh *et al*., 2000). Conversely, TNF$^{-/-}$ and TNFR2$^{-/-}$ mice (the latter lacking the receptor preferentially activated by transmembrane TNF) develop worse EAE and show significantly impaired remyelination (Liu *et al*., 1998; Eugster *et al*., 1999; Suvannavejh *et al*., 2000; Arnett *et al*., 2001). In an elegant study with knock-in mice expressing transmembrane TNF only, Alexopoulou *et al*. (2006) demonstrated that transmembrane TNF is sufficient to suppress both induction and chronic phases of EAE as well as anti-myelin autoimmune reactivity, while maintaining antimicrobial host defences (Alexopoulou *et al*., 2006). Collectively, these studies illustrate how the general understanding of TNF involvement in multiple sclerosis has profoundly evolved over the past decade: from the dogma that TNF, as a whole, is a key pathological mediator in multiple sclerosis, to recognizing that two distinct forms of TNF exist, soluble TNF and transmembrane TNF, and that multiple sclerosis pathology is associated with a detrimental effect of soluble TNF (Kassiotis and Kollias, 2001).

Given the contrasting and often confusing data in the literature, we sought to investigate the distinct roles of soluble TNF and transmembrane TNF in the development of EAE using a pharmacological approach, hypothesizing that if selective pharmacological inhibition of soluble TNF without interfering with transmembrane TNF proved efficacious in a model of multiple sclerosis, we could have a candidate for immediate translation into multiple sclerosis therapy. We employed a new biologic, XPro1595, which selectively inhibits soluble TNF without affecting transmembrane TNF. XPro1595 is the leading compound of a novel class of dominant-negative TNF biologics that, by rapidly exchanging subunits with native soluble TNF but not membrane-anchored transmembrane TNF, form inactive mixed heterotrimers eliminating soluble TNF activity without inhibiting transmembrane TNF (Steed *et al*., 2003; Zalevsky *et al*., 2007; Olleros *et al*., 2009). We compared the effects of XPro1595 to those of the non-selective TNF inhibitor etanercept [decoy TNFR2 which blocks soluble TNF, transmembrane TNF and lymphotoxin (Goffe and Cather, 2003)] and found that inhibition of soluble TNF by XPro1595 is therapeutic in myelin oligodendrocyte glycoprotein (MOG)-induced EAE,

whereas non-selective inhibition of both soluble TNF and transmembrane TNF by etanercept is not. Mice treated with XPro1595 recover from paralysis and display significant axonal preservation and remyelination. Our studies underscore the opposing roles of soluble TNF and transmembrane TNF in the pathophysiology of EAE, and suggest that the protective effects of TNF in chronic disease are mediated by transmembrane TNF. We show that by inhibiting soluble TNF while preserving transmembrane TNF signalling, we can positively modulate two essential processes for maintaining and improving function in multiple sclerosis, neuroprotection and remyelination, not only opening a new avenue of therapy for the treatment of multiple sclerosis, but also helping to reconcile the apparently conflicting findings emerged from animal models and clinical trials (Caminero *et al.*, 2011).

Materials and methods

Mice

Experiments were performed according to the protocols approved by the Institutional Animal Care and Use Committee of the University of Miami. Female C57BL/6 mice 2- to 4-months-old were obtained from Jackson Laboratories. Animals were housed in a virus/antigen-free facility with a 12 h light/dark cycle, controlled temperature and humidity, and provided with water and food *ad libitum*.

Induction of experimental autoimmune encephalomyelitis and pharmacological treatments

Active EAE was induced with $MOG_{(35–55)}$ peptide purchased from BioSynthesis Inc., as previously described (Szalai *et al.*, 2002; Brambilla *et al.*, 2009). Clinical signs of EAE were assessed daily using a standard scale of 0–6 as follows: 0, no clinical signs; 1, loss of tail tone; 2, fully flaccid tail; 3, complete hind limb paralysis; 4, complete forelimb paralysis; 5, moribund; 6, dead. XPro1595 [formerly XENP1595 (Zalevsky *et al.*, 2007), Xencor Inc.] and etanercept (Enbrel®, Amgen-Wyeth) were administered subcutaneously at a dose of 10 mg/kg every 3 days beginning at Day 16, when at least half of the mice had reached a clinical score $\geqslant 2$.

Isolation of leucocytes from spinal cord and spleen

Cells were isolated as previously described (Brambilla *et al.*, 2009). Briefly, spinal cords and spleens were homogenized into single cell suspensions through a 70-μm mesh cell strainer. For isolation of infiltrating leucocytes into the spinal cord, spinal cord suspensions were spun at 400*g* for 5 min. After removal of supernatants, cells were collected, resuspended in 40% Percoll, layered on 70% Percoll and centrifuged at 400*g* for 25 min at room temperature. Cells at the gradient interface were removed, washed in fluorescence-activated cell sorting buffer (eBioscience) and stained as described below. For leucocyte isolation from the spleen, suspensions were spun at 400*g* for 5 min. After removal of supernatants, red blood cells were lysed in 1 ml lysis buffer (eBioscience) according to the manufacturer's instructions. Cells were then resuspended in fluorescence-activated cell sorting buffer and stained as described below. Spinal cords from seven to eight animals were pooled to obtain a sufficient number of cells for flow cytometry analysis. Spleens from individual animals were evaluated separately.

Staining and flow cytometry

Cells were incubated on ice for 10 min with anti-CD16/32 (FcR block, eBioscience) to prevent non-specific staining and subsequently stained for 30 min at 4°C with: PE-Cy7-anti-CD45 (1:10 000); AlexaFluor488-anti-CD3, Pacific Blue- or PE-anti-CD4 (1:200); APC-anti-CD8 (1:200); APC-AlexaFluor750-anti-B220 (1:200); PE-anti-NK1.1 (1:200); and eFluor450-CD11b (1:200), from eBioscience. Cell suspensions were fixed overnight in 1% paraformaldehyde in fluorescence-activated cell sorting buffer and analysed with an LSR II flow cytometer equipped with FACSDiva 6.0 software (BD Biosciences).

Mouse tissue immunohistochemistry

Animals were perfused with 4% paraformaldehyde in 0.1 M phosphate-buffered saline. Tissues were cryoprotected in 0.1 M phosphate-buffered saline + 25% sucrose and cryostat-cut into 15 or 30 μm thick sections. After blocking for 1 h with 5% normal goat serum in 0.1 M phosphate-buffered saline + 0.4% Triton-X, sections were incubated overnight at 4°C with primary antibodies against GFAP (rabbit, 1:1000, Dako; mouse, 1:1000, BD Biosciences), CD45 (rat, 1:200, eBioscience), NG2 (rabbit, 1:500, Millipore), TNFR1 (rabbit, 1:50, or mouse, 1:50, Santa Cruz), TNFR2 (rabbit, 1:50, or mouse, 1:50, Santa Cruz), MAP2 (mouse, 1:1000, Sigma), CD11b (rat, 1:100, Serotec) and CC1 (mouse, 1:500, Calbiochem). Immunoreactivity was visualized either with secondary species-specific fluorescent antibodies (AlexaFluor-594 and -488, Invitrogen) or with 3-3′diaminobenzidine staining using the Vector Elite ABC kit (Vector Labs) according to the manufacturer's instructions. Images were obtained with an Olympus FluoView 1000 confocal microscope or with a Zeiss Axiovert 200 M fluorescence microscope.

Quantification of $NG2^+$ cells

Following immunolabelling with anti-NG2 antibody as described above, quantification of the total numbers of $NG2^+$ cells was determined applying principles of stereology. Briefly, 10 serial sections taken at 150 μm intervals and with a thickness of 30 μm were analysed, and the cells of interest manually counted on each section at ×63 magnification. The total number of positive cells per cubic millimetre of tissue was estimated with Stereoinvestigator software (MicroBrightField, Inc.). For these assessments, six animals per group were used.

Toluidine blue staining and electron microscopy tissue preparation

After perfusion, 1 mm segments of the thoracic spinal cord were fixed in 2% glutaraldehyde/100 mM sucrose and rinsed in 0.15 M phosphate buffer before post-fixing with 2% OsO_4 for 1 h. Following dehydration in graded ethanol solutions, tissues were embedded in epoxy resin (Embed, Electron Microscopy Sciences). Semi-thin sections (1 μm thick) were obtained with a Leica Ultracut E microtome and stained with 1% toluidine blue solution. Samples were then examined by light microscopy or using a Philips CM-10 transmission electron microscope. The number of toluidine blue-stained myelinated axons was estimated

using the software Stereoinvestigator. For this assessment, six animals per group were used.

Quantification of *g*-ratios on electron microscopy micrographs

For assessment of the *g*-ratio (axon diameter/fibre diameter) of axons in the thoracic spinal cord, electron microscopy micrographs were taken at a magnification of ×52 000 with a Philips CM-10 transmission electron microscope. A grid was placed over the section and pictures taken randomly from each quadrant corresponding to the lateral columns of the cord. One picture per quadrant was evaluated for a minimum of 30 images per mouse. On each micrograph, fibre diameter and axon diameter of each single axon were manually measured. Due to the irregular shape of the elements, the approximate diameter was calculated as the average of three diameters measured for each element. For this assessment, six animals per group were used.

Total RNA isolation and real-time reverse-transcriptase polymerase chain reaction

Total RNA was extracted with TRIZOL® according to the manufacturer's instructions (Invitrogen). To ensure complete elimination of genomic DNA, RNA was further purified with RNeasy® MinElute Cleanup Kit (Qiagen) in combination with DNA digestion using RNase-free DNase (Qiagen). Reverse transcription was performed with Superscript® II (Invitrogen), according to the manufacturer's protocols. Complementary DNA equal to 10–50 ng of initial total RNA was used as a template in each polymerase chain reaction. Real-time polymerase chain reaction was performed in the Rotor-Gene 3000 Real Time Cycler (Corbett Life Science) with QuantiTect® SYBR® Green PCR MasterMix (Qiagen). Relative expression was calculated by comparison with a standard curve, after normalization to glyceraldehyde-3-phosphate dehydrogenase and β-actin gene expression. Primers for gene amplification are listed in Supplementary Table 3.

Western blotting

Proteins were resolved by sodium dodecyl sulphate–polyacrylamide gel electrophoresis on 6–15% gels, transferred to nitrocellulose and blocked in 5% non-fat milk. Membranes were probed with antibodies against: CD45 (rat, 1:1000, eBioscience); neurofilament-H (rabbit, 1:1000, Serotec); neurofilament-H non-phosphorylated (SMI32; mouse, 1:1000, Covance); GFAP (mouse, 1:1000, BD Pharmingen); glyceraldehyde-3-phosphate dehydrogenase (mouse, 1:2000, Imgenex), followed by horseradish peroxidase-conjugated secondary antibodies. Proteins were visualized with ECL (GE Healthcare/Amersham) and bands quantified with Quantity One® software (Biorad). Data were normalized against glyceraldehyde-3-phosphate dehydrogenase and expressed as per cent of vehicle.

Histological analysis of human spinal cords with progressive multiple sclerosis

Tissue sampling

The study was performed on post-mortem spinal cord tissue from two cases with secondary progressive multiple sclerosis and one case with primary progressive multiple sclerosis obtained from the UK Multiple Sclerosis Tissue Bank at Imperial College, London (see Supplementary Table 2 for demographic, clinical and neuropathological data). All multiple sclerosis tissues were obtained via a UK prospective donor scheme with full ethical approval (08/MRE09/31). One tissue block (4 cm^2 surface area) was randomly selected for each case based on images taken at the time of dissection, without prior knowledge of the presence of white matter or grey matter lesions. Serial sections were then processed by immunohistochemistry in order to determine cell-specific expression of TNFR1 and TNFR2.

3,3′-Diaminobenzidine immunohistochemistry

Air dried, acetone fixed, 10 μm-thick cryosections (cut from the 4% paraformaldehyde fixed tissue blocks) were rehydrated with phosphate-buffered saline and subjected to antigen retrieval procedure (microwave treatment in 10 mM citrate buffer, pH 6.0). Sections were then incubated for 30 min with 0.1% H_2O_2 in phosphate-buffered saline to eliminate endogenous peroxidase activity, for 1 h with 10% normal serum, and overnight at 4°C with primary antibodies against TNFR1 (mouse, 1:50; Serotec) or TNFR2 (rabbit, 1:50; Sigma) diluted in phosphate-buffered saline containing 0.2% Triton 100-X and 1% bovine serum albumin or 1% normal serum. Binding of biotinylated secondary antibodies (Jackson Immunoresearch Laboratories) was visualized with the avidin–biotin horseradish peroxidase complex (ABC Vectastain Elite kit, Vector Laboratories) followed by 3,3′-diaminobenzidine (Sigma) as substrate. All sections were counterstained with haematoxylin, sealed with DePeX polystyrene and viewed under a Zeiss Axiophot microscope equipped with a digital camera (Axiocam MRC). Images were acquired using Axiovision 4 AC software. Negative controls included IgG isotype antibodies or preimmune serum or omission of the primary antibody.

Immunofluorescent staining

After post-fixation in cold acetone, sections were blocked with 5–10% normal serum in phosphate-buffered saline, and incubated overnight at 4°C with primary antibodies diluted in phosphate-buffered saline containing 0.2% Triton X-100 and 1% normal serum. Double-immunofluorescent labelling was conducted with anti-TNFR1 or anti-TNFR2 antibodies in combination with antibodies against: MAP2 (1:300, Dako), CNPase (1:100, Chemicon), GFAP (1:300, Dako), MHC class II (1:50, Dako) or IBA1 (1:300, Abcam). Sections were then incubated with Cy3-, rhodamine- or fluorescein-conjugated species-specific secondary antibodies in phosphate-buffered saline containing 1% normal serum for 1 h. Some sections were counterstained with DAPI (Sigma) for localization of cell nuclei. Finally, sections were coverslipped with Vectashield® mounting medium (Vector Laboratories). For negative controls, the primary antibodies were replaced with preimmune serum or IgG isotype controls. Slides were viewed under epifluorescence microscope (Leica Microsystem).

Statistical analysis

Statistical analysis of the clinical course of EAE was carried out with the Mann–Whitney test. Real-time polymerase chain reaction and western blot data were analysed with one-way ANOVA followed by Tukey's test for multiple comparisons. For single comparisons, Student's *t*-test was applied. $P \leqslant 0.05$ were considered statistically significant.

Results

Inhibition of soluble TNF with XPro1595 improves functional recovery after MOG-induced experimental autoimmune encephalomyelitis

To dissect the roles of soluble TNF and transmembrane TNF in EAE, we analysed in parallel the effect of XPro1595, a selective soluble TNF inhibitor (Zalevsky *et al*., 2007; Olleros *et al*., 2009), and etanercept, a non-selective TNF inhibitor (Goffe and Cather, 2003; Tracey *et al*., 2008), on $MOG_{(35–55)}$-induced EAE in C57BL/6 female mice. Both biologics have comparable efficacy and potency (Zalevsky *et al*., 2007) and contrary to other anti-TNF options, which are structurally anti-human antibodies (e.g. infliximab, adalimumab, certolizumab pegol), they are effective in murine models. We chose a clinically relevant treatment protocol starting administration at 16 days post-induction of disease, when at least half the animals displayed acute symptoms of EAE (score $\geqslant 2$). Treatment at a dose of 10 mg/kg was repeated every 3 days until sacrifice (55 days post-induction). All groups reached peak disease in a similar fashion, but animals treated with XPro1595 exhibited markedly improved functional recovery compared with vehicle- and etanercept-treated mice (Fig. 1A), with maximum improvement achieved around Day 25 and maintained throughout the remainder of the experiment. From Day 25 onwards, XPro1595-treated mice scored consistently <1.5, which signifies only mild flaccidity of the tail without any sign of hindlimb or forelimb paralysis. The overall attenuation of the pathology is also reflected in the significant reduction in cumulative disease index (Table 1). On the contrary, etanercept-treated mice did not show amelioration but rather chronic exacerbation of disease similarly to control (vehicle) mice (Fig. 1A). Chronically, both groups scored well >2.0, showing hindlimb and forelimb paralysis at various degrees of severity. It is noteworthy that treatment with either compound did not alter TNFR1 or TNFR2 protein expression in the CNS (Supplementary Fig. 1), indicating that no compensatory expression of these receptors was induced as a consequence of the pharmacological inhibition.

The therapeutic effect of soluble TNF inhibition with XPro1595 is not solely dependent on modulation of the acute immune-inflammatory response

In order to evaluate whether the therapeutic effect of XPro1595 could be associated with changes in the immune response to MOG immunization in the periphery or in the spinal cord, we analysed the distribution of leucocyte populations by flow cytometry in spleen and spinal cord preparations at acute (28 days post-induction) and chronic (55 days post-induction) disease (Table 2). In the spleen at both time points, XPro1595 and etanercept had no effect on the relative percentages of B cells ($B220^+$), T cells ($CD3^+$) and macrophages ($CD11b^+$) compared with the vehicle group. The only significant differences, although minimal, were a small reduction in $CD4^+$ and increase in $CD8^+$ T cells. In the spinal cord, at acute disease, we detected a marked attenuation in $CD45^{high}CD11b^+$ infiltrating macrophages, as well as in $CD45^{low}CD11b^+$ microglia both in XPro1595- and etanercept-treated groups compared with vehicle (Fig. 1B, Table 2). This effect appeared comparable between XPro1595- and etanercept-treated groups, suggesting that the long-term functional recovery observed with XPro1595 cannot be solely dependent on inhibition of acute macrophage infiltration in the CNS or of microglia activation. At chronic disease, leucocyte infiltrates into the spinal cord were almost undetectable in all groups, rendering flow cytometry analysis experimentally unfeasible. Immunohistochemically, we detected the presence of sporadic $CD45^+$ cells in subpial regions of the white matter in all conditions, without appreciable differences between treatments (Fig. 1C). This was confirmed by western blot analysis of CD45 protein expression (Fig. 1D), showing no significant differences among groups. Interestingly, in XPro1595-treated mice we measured a significantly reduced expression of GFAP by immunohistochemistry and western blot (Fig. 1C and D), indicating attenuated astroglial reactivity compared with vehicle- and etanercept-treated mice. It has been shown with genetic models that inhibition of astrogliosis and astrocyte-dependent inflammation is protective against EAE (van Loo *et al*., 2006; Brambilla *et al*., 2009), hence it is plausible that by blocking soluble TNF signalling with XPro1595 we can elicit a dampening effect, direct or indirect, on astrocyte activation, obtaining with our pharmacological approach a similar effect to that observed in transgenic mice.

Inhibition of both soluble and transmembrane TNF reduces expression of proinflammatory cytokines and chemokines after MOG-induced experimental autoimmune encephalomyelitis

To further investigate whether the therapeutic effect of XPro1595 was dependent on a reduction of the inflammatory response, we evaluated the expression of proinflammatory cytokines and chemokines at chronic disease (55 days post-induction). We found that both XPro1595 and etanercept significantly reduced expression of IFNγ, TNF, IL1β, IL6 and CCL2 compared with the vehicle-treated mice (Fig. 2), providing further demonstration that the therapeutic outcome of soluble TNF inhibition is not exclusively dependent on attenuation of the inflammatory response. Indeed, a reduction of the inflammatory response occurs similarly in etanercept-treated mice, but is not sufficient to produce functional improvement. XPro1595 treatment also reduced expression of CCL5, CXCL10 and CCR2 compared with vehicle, while etanercept did not, suggesting that transmembrane TNF signalling could be associated with a specific anti-inflammatory and repair signature.

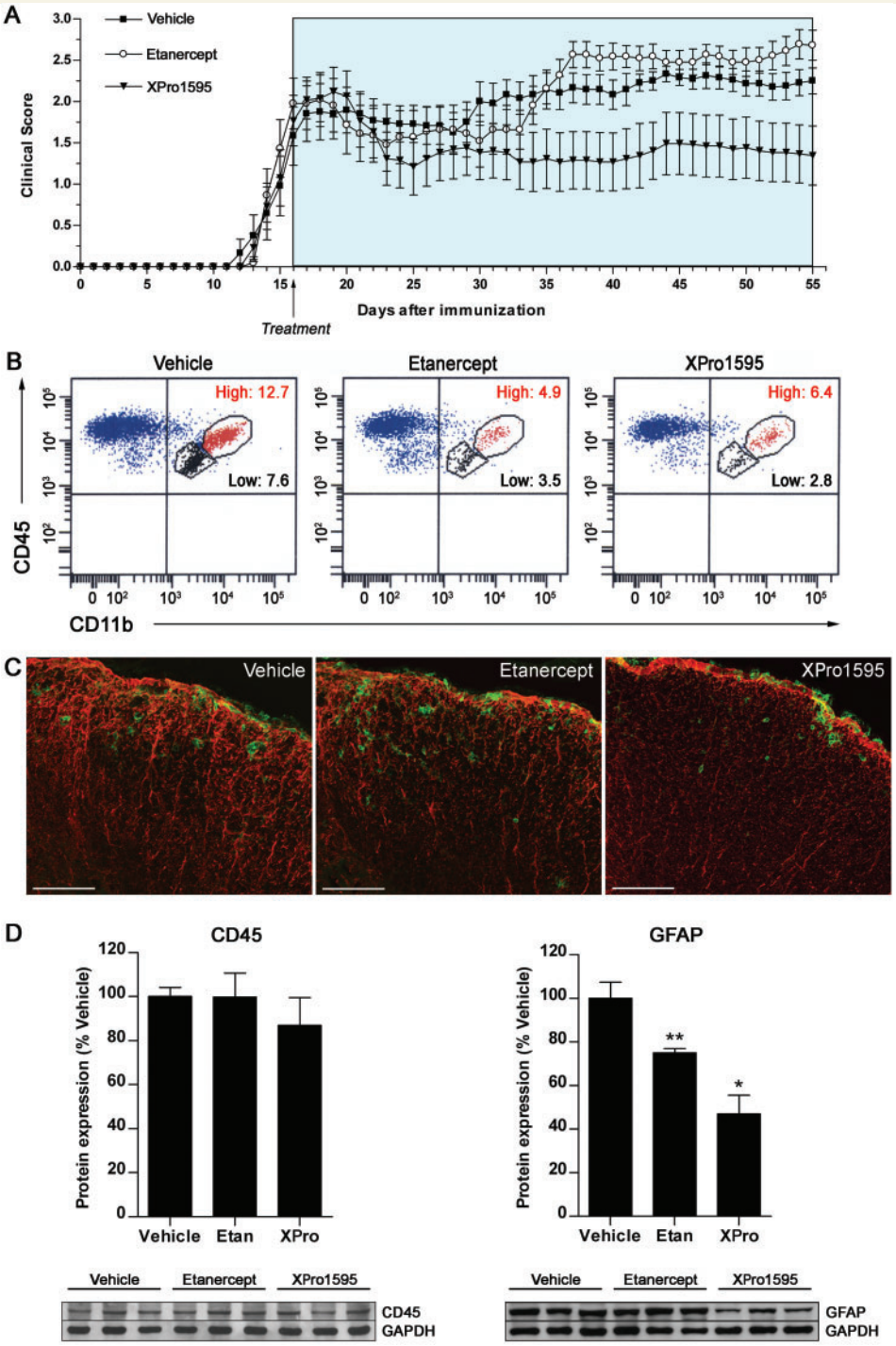

Figure 1 Treatment with XPro1595 improves functional outcome in MOG-induced EAE. (**A**) Clinical course of $MOG_{(35–55)}$-induced EAE in mice treated with vehicle (saline), etanercept or XPro1595. Treatment with pharmacological agents was initiated at Day 16, when at least half of the animals reached a minimum clinical score of 2. Both etanercept and XPro1595 were administered at a dose of 10 mg/kg every 3 days until the end of the experiment (55 days post-induction). Results are expressed as the daily mean clinical score ± SEM of 13–15 animals/group from two independent experiments. The XPro1595 curve is significantly different from both vehicle and etanercept curves ($P < 0.0001$, Mann–Whitney test). (**B**) Flow cytometry analysis of microglia ($CD45^{low}CD11b^{+}$ population, black dots) and infiltrating macrophages ($CD45^{high}CD11b^{+}$ population, red dots) in the spinal cord of vehicle-, etanercept- and XPro1595-treated mice at acute disease (28 days post-induction). A representative experiment is shown, obtained by sampling eight animals per group. (**C**) Double immunostaining for CD45 (green) and GFAP (red) in the thoracic spinal cord of vehicle-, etanercept- and XPro1595-treated mice at chronic disease (55 days post-induction); scale bar = 100 μm. (**D**) Quantification of CD45 and GFAP protein expression in spinal cord tissue of vehicle-, etanercept- and XPro1595-treated mice at 55 days post-induction. Data are normalized to glyceraldehyde-3-phosphate dehydrogenase (GAPDH) protein expression. Representative experiments are shown. Results, expressed as per cent of vehicle, are the mean ± SEM of five animals per group. $^{*}P < 0.05$ versus vehicle and etanercept; $^{**}P < 0.05$ versus vehicle by one-way ANOVA with Tukey's test.

Inhibition of soluble TNF with XPro1595 promotes axon preservation after MOG-induced experimental autoimmune encephalomyelitis

Histological analysis of the thoracic spinal cord of naïve and EAE-induced mice (55 days post-induction) showed a more prevalent axonal damage in the lateral and posterior funiculi. Clear axon preservation was observed in the XPro1595 group compared with vehicle and etanercept (Fig. 3A), which both displayed a high frequency of enlarged, swollen and hypomyelinated axons, as well as fully collapsed (black arrows) axons. When counting the number of myelinated axons in the white matter, we found a significantly higher number in the XPro1595 group (24800 ± 2477 axons/mm^2) compared with vehicle (16681 ± 1528 axons/mm^2) and etanercept (17556 ± 1295 axons/mm^2) (Fig. 3B). Collapsed axons (obliterated, hence non-functional) were also reduced in XPro1595-treated mice (992 ± 314 collapsed axons/mm^2) compared with vehicle- (1958 ± 399 collapsed axons/mm^2) and etanercept-treated (2842 ± 585 collapsed axons/mm^2) mice (Fig. 3C). Interestingly, no differences were found among all groups in the number of infiltrating leucocytes (Fig. 3D), in agreement with previously shown CD45 immunohistochemistry and protein expression data (Fig. 1C and D).

To further substantiate the observation that XPro1595 treatment promotes axonal preservation, we evaluated expression of the axon-specific molecule neurofilament-H. *Neurofilament-H* gene and protein expression were increased in the XPro1595-treated group compared with vehicle (Fig. 3E), and vehicle and etanercept (Fig. 3F), respectively. On the other hand, the non-phosphorylated form of neurofilament-H, commonly associated with axonal damage (Trapp *et al.*, 1998), was significantly reduced in XPro1595-treated mice compared with etanercept (Fig. 3G). Together these data point to a neuroprotective effect of XPro1595 following EAE.

Table 1 Clinical parameters of EAE

Group	Incidence (%)	Onset (day)	Cumulative disease index
Vehicle	85.7 (12 of 14)	18.33 ± 1.63	83.33 ± 6.08
Etanercept	84.6 (11 of 13)	18.45 ± 2.13	87.67 ± 6.93
XPro1595	86.7 (13 of 15)	18.17 ± 2.30	60.41 ± 9.02*

Results represent the mean ± SEM of 13–15 animals per group from two independent experiments. Onset is considered when animals reach a clinical score of 2 for two consecutive days. Cumulative Disease Index is calculated as the sum of the clinical scores of each animal between Day 7 and Day 55 and is a measure of disease severity. *$P < 0.005$ versus vehicle and etanercept, Student's *t*-test.

Inhibition of soluble TNF with XPro1595 preserves myelin compaction after MOG-induced experimental autoimmune encephalomyelitis

To address whether XPro1595-mediated neuroprotection was associated with a direct effect on myelin preservation, we analysed

Table 2 Flow cytometric analysis of leucocyte profiles in spleen and spinal cord of vehicle-, etanercept- and XPro1595-treated mice at 28 and 55 days post-induction

Spleen	CD45 gate			CD3 gate	
	B cells (B220$^+$)	T cells (CD3$^+$)	Macrophages (CD11b$^+$)	CD4$^+$	CD8$^+$
28 days post-induction					
Vehicle	28.2 ± 0.9	23.9 ± 0.7	43.1 ± 1.1	60.2 ± 0.9	34.4 ± 1.0
Etanercept	28.8 ± 3.6	21.4 ± 0.7	45.4 ± 4.5	55.7 ± 1.7*	39.9 ± 1.6*
XPro1595	24.1 ± 1.5	21.0 ± 1.4	50.7 ± 3.0	57.1 ± 1.4	38.8 ± 1.3*
55 days post-induction					
Vehicle	28.2 ± 2.0	48.7 ± 1.9	9.9 ± 1.1	61.5 ± 0.7	31.2 ± 1.2
Etanercept	28.9 ± 2.9	50.9 ± 3.4	8.9 ± 0.9	63.4 ± 1.0	32.9 ± 1.4
XPro1595	30.0 ± 1.5	49.0 ± 1.8	8.9 ± 0.8	61.0 ± 0.9	31.2 ± 1.2

Spinal cord	CD45 gate			
	CD4$^+$	CD8$^+$	CD45^{high}CD11b$^+$ (Macrophages)	CD45^{low}CD11b$^+$ (Microglia)
28 days post-induction				
Vehicle	40.8	24.3	12.7	7.6
Etanercept	49.1	25.1	4.9	3.5
XPro1595	45.4	31.8	6.4	2.8

For the spinal cord, results represent the mean of two independent experiments each conducted by pooling eight animals per group. For the spleen, each animal was evaluated individually and results represent the mean of 8–10 mice from two independent experiments. *$P < 0.05$ versus vehicle, Student's *t*-test.

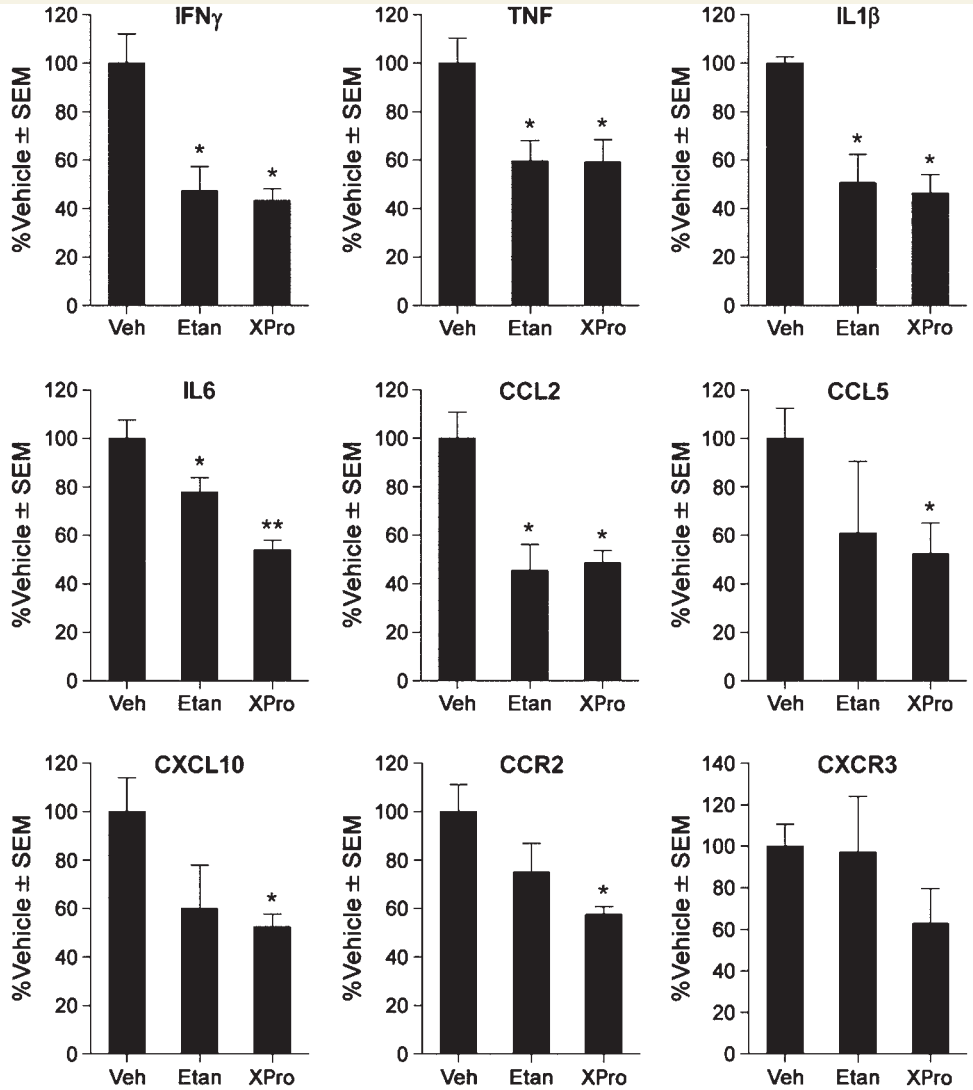

Figure 2 Profile of cytokine and chemokine gene expression 55 days after induction of EAE. Differential expression of cytokines and chemokines was evaluated in spinal cord tissue of vehicle- (Veh), etanercept- (Etan) and XPro1595-treated mice at 55 days post-induction. For each gene, results are expressed as per cent of vehicle ± SEM after normalization to glyceraldehyde-3-phosphate dehydrogenase gene expression. Five animals/group were analysed. *$P < 0.05$ versus vehicle; **$P < 0.05$ versus vehicle and etanercept by one-way ANOVA with Tukey's test.

myelin compaction by electron microscopy. As expected, all EAE-induced groups (Fig. 4B–D and F–H) showed signs of 'loose' myelin compared with naïve mice (Fig. 4A and E). Significant damage was especially evident in vehicle- and etanercept-treated mice, where blebbing, loss of adaxonal contact and unravelling of the myelin sheaths were prevalent. Lipid inclusions in the axoplasm, a sign of axonal damage, were also found. In the XPro1595-treated group, however, myelin compaction appeared rather preserved, as indicated by more tightly associated myelin layers (Fig. 4H) compared with vehicle- and etanercept-treated groups (Fig. 4F and G). These observations were confirmed by quantification of the *g*-ratio (axon diameter/fibre diameter), which was significantly higher for all diameter sizes in XPro1595-treated mice compared with vehicle and etanercept groups, and similar to naïve mice (Fig. 4I).

Inhibition of soluble TNF with XPro1595 promotes remyelination after MOG-induced experimental autoimmune encephalomyelitis

We used electron microscopy to investigate whether inhibition of soluble TNF could have an effect on remyelination, increasing the potential for properly functioning axons. We counted remyelinating axons based on morphological characteristics (Fig. 5A) and found a significantly higher number in the XPro1595-treated group compared with vehicle and etanercept (Fig. 5B). As expected, all groups had more remyelinating axons than uninjured naïve mice. Interestingly, not only did XPro1595 promote remyelination, but it supported remyelination of larger diameter axons.

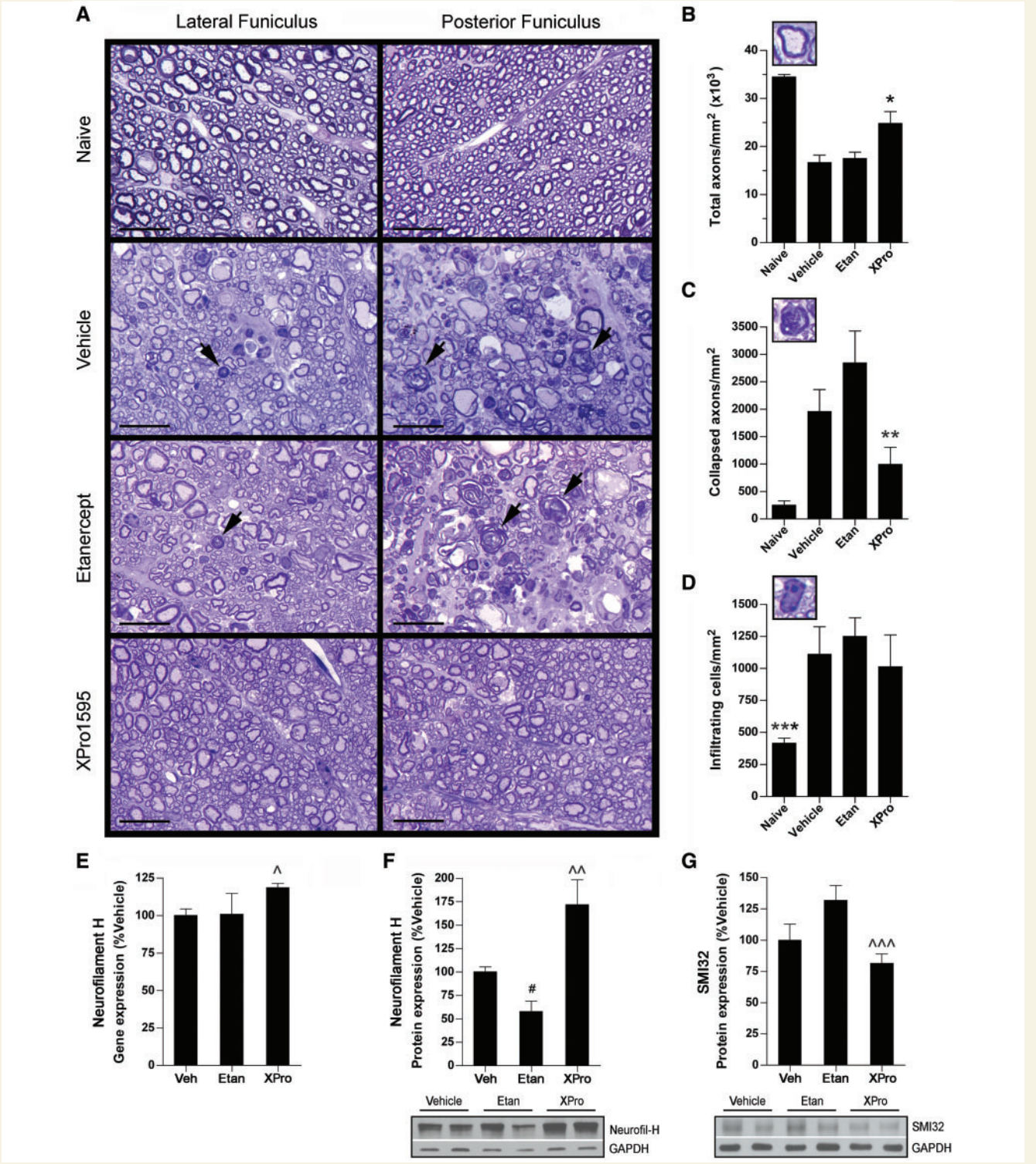

Figure 3 Treatment with XPro1595 improves axonal preservation in MOG-induced EAE. (**A**) Toluidine blue staining of ultrathin sections of the thoracic spinal cord of naïve, vehicle-, etanercept- and XPro1595-treated mice at 55 days post-induction. Black arrows indicate collapsed obliterated axons (scale bar = 10 μm). (**B**) Quantification of toluidine blue-stained myelinated axons, (**C**) collapsed axons and (**D**) infiltrating immune cells in the spinal cord white matter: $*P < 0.05$ versus naïve, vehicle and etanercept; $**P < 0.05$ versus vehicle and etanercept; $***P < 0.05$ versus vehicle, etanercept and XPro1595, unpaired *t*-test. (**E**) Real-time polymerase chain reaction quantification of neurofilament-H gene expression; western blot quantification of neurofilament H (**F**) and SMI32 (**G**) protein expression: $^P < 0.05$ versus vehicle; $^^P < 0.05$ versus vehicle and etanercept; $^{\#}P < 0.05$ versus XPro1595; $^^^P < 0.05$ versus etanercept, unpaired *t*-test. Six animals per group were analysed.

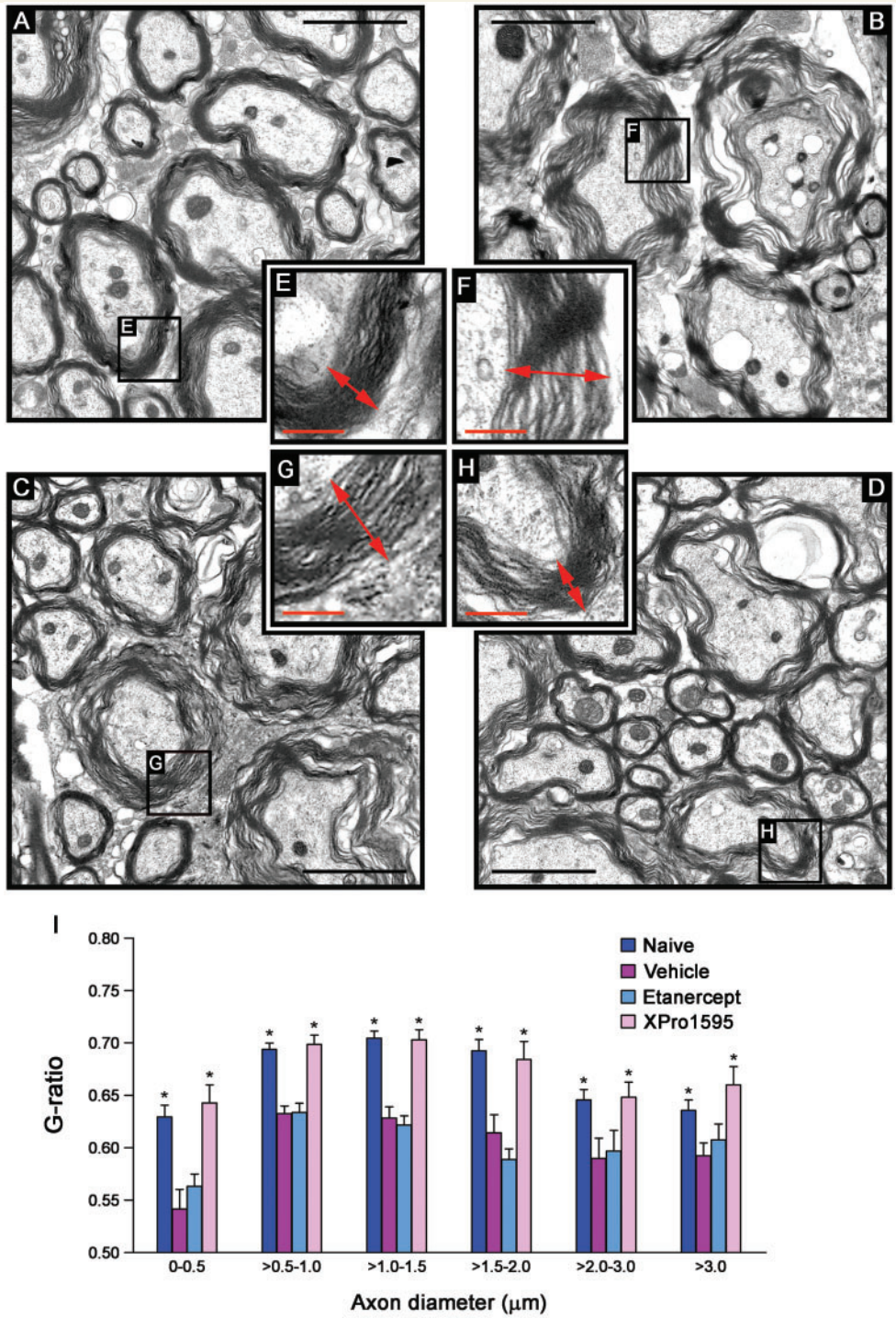

Figure 4 Treatment with XPro1595 improves myelin compaction after MOG-induced EAE. (**A–H**) Electron micrographs of the lateral columns of the thoracic spinal cord comparing naïve mice (**A** and **E**) to vehicle- (**B** and **F**), etanercept- (**C** and **G**) and XPro1595- (**D** and **H**) treated mice at 55 days post-induction. Red arrows show the average thickness of the myelin sheaths in representative myelinated axons of comparable diameter from the various treatments groups. Red scale bars = 0.5 μm; black scale bars = 2 μm. **(I)** Quantification of the *g*-ratios (axon diameter/fibre diameter) of myelinated fibres grouped by increasing axon diameter. $^*P < 0.05$ versus vehicle and etanercept by one-way ANOVA with Tukey's test.

Indeed, the percentage of remyelinating axons with diameter >1 μm was significantly higher following treatment with XPro1595 (Fig. 5C). Because these larger axons are primarily motor fibres, rather than sensory, their remyelination is highly relevant for motor function recovery. Increased remyelination was also accompanied by higher expression of myelin-specific

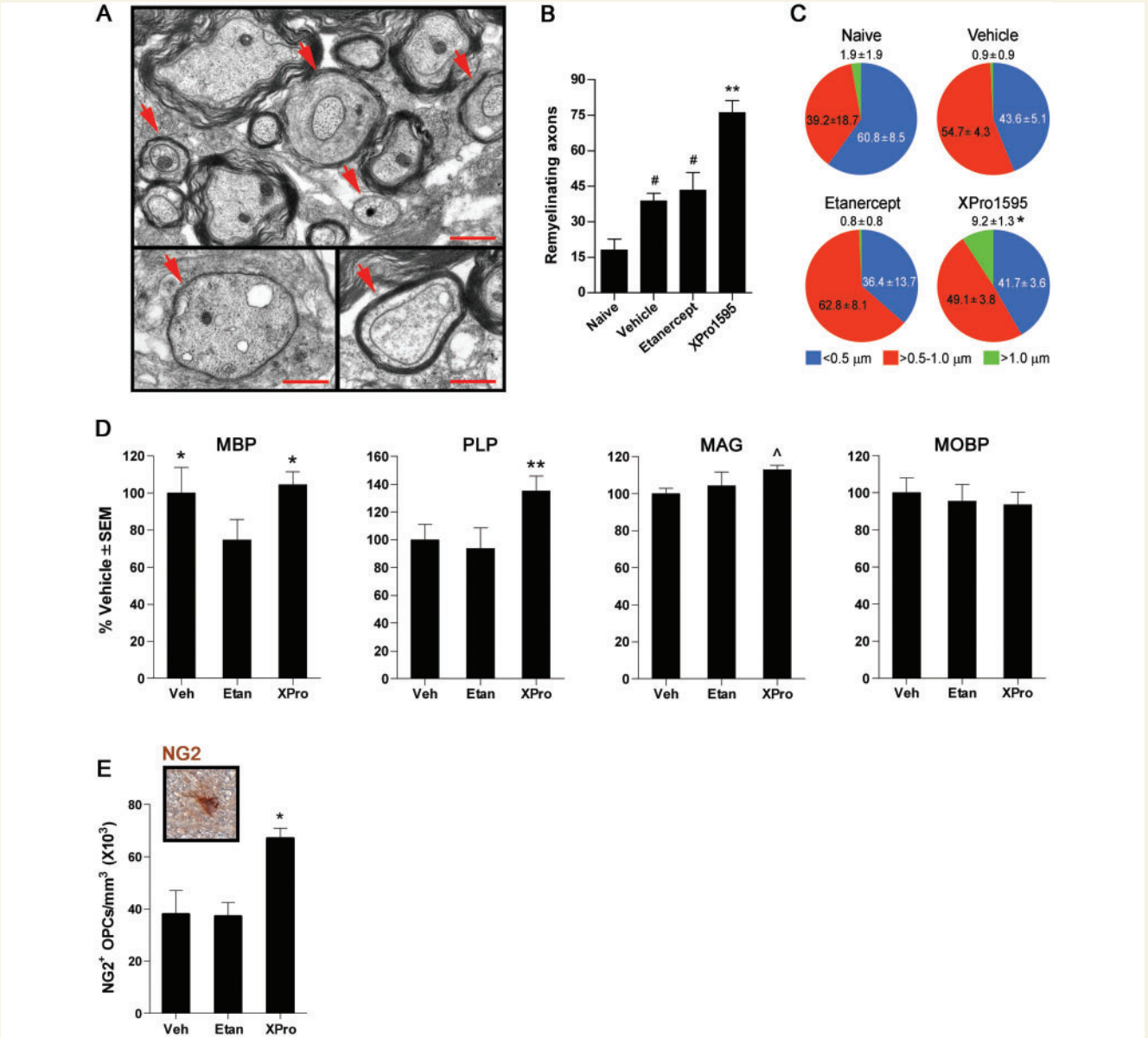

Figure 5 Treatment with XPro1595 promotes remyelination after MOG-induced EAE. (**A**) Electron micrographs of remyelinating axons (red arrows) in the thoracic spinal cord of XPro1595-treated mice at 55 days post-induction. Scale bars = 1 µm. (**B**) Quantification of remyelinating axons in the thoracic spinal cord of naïve, vehicle-, etanercept- and XPro1595-treated mice at 55 days post-induction. $^{**}P < 0.05$ versus naïve, vehicle and etanercept; $^{\#}P < 0.05$ versus naïve and XPro1595 by one-way ANOVA with Tukey's test. (**C**) Size distribution of remyelinating axons in naïve, vehicle-, etanercept- and XPro1595-treated mice at 55 days post-induction; results are expressed as per cent of the total number of remyelinating axons ± SEM; $^{*}P < 0.05$ versus corresponding naïve, vehicle and etanercept by one-way ANOVA with Tukey's test. (**D**) Quantification of the expression of myelin genes at 55 days post-induction. Results are expressed as per cent of vehicle ± SEM following normalization to glyceraldehyde-3-phosphate dehydrogenase; $^{*}P < 0.05$ versus etanercept, $^{**}P < 0.05$ versus vehicle and etanercept, $^{\wedge}P < 0.05$ versus vehicle by one-way ANOVA with Tukey's test. (**E**) Quantification of $NG2^+$ oligodendrocyte precursor cells in the spinal cord white matter of vehicle-, etanercept- and XPro1595-treated mice at 55 days post-induction. $^{*}P < 0.05$ versus vehicle and etanercept by unpaired *t*-test. MAG = myelin associated glycoprotein; MBP = myelin basic protein; MOBP = myelin-associated oligodendrocyte basic protein; PLP = proteolipid protein.

proteins, particularly proteolipid protein, the predominant myelin protein in the CNS, which was upregulated in XPro1595-treated animals compared with both vehicle- and etanercept-treated mice (Fig. 5D). Myelin basic protein and myelin-associated glycoprotein levels were significantly higher in XPro1595-treated mice compared with etanercept, and vehicle and etanercept, respectively (Fig. 5D).

Finally, to determine if the pro-myelinating effect of XPro1595 could be associated with a modulation of the number of oligodendrocyte precursor cells, we counted $NG2^+$ oligodendrocyte

precursor cells in the spinal cord white matter of EAE-induced mice and found a significant increase in the XPro1595-treated group compared with the others. This opens the possibility that transmembrane TNF activates mechanisms leading to proliferation and/or survival of precursors, increasing the pool of cells ready to mature into new myelinating oligodendrocytes.

TNFR1 and TNFR2 expression profiles in the mouse spinal cord at acute experimental autoimmune encephalomyelitis

To begin evaluating the possible mechanisms associated with the beneficial effects of transmembrane TNF in EAE, we performed an in-depth expression study analysing by confocal microscopy, TNFR1 and TNFR2 cell-specific distribution in the mouse spinal cord at the acute phase of EAE. TNFR1 was found to be highly expressed in neurons, particularly in cluster-like structures along MAP2$^+$ dendrites in the grey matter (Fig. 6). Expression was also detected on GFAP$^+$ astrocytes and CC1$^+$ oligodendrocyte cell bodies, mainly in the white matter. Conversely, NG2$^+$ oligodendrocyte precursor cells and CD11b$^+$ microglia/macrophages appeared devoid of TNFR1 (Fig. 6). As for TNFR2 (Fig. 7), no specific immunoreactivity was found on MAP2$^+$ neurons, contrary to TNFR1. TNFR2 expression was instead detected on GFAP$^+$ astrocytes (with high levels in the white matter), CC1$^+$ oligodendrocytes and NG2$^+$ oligodendrocyte precursor cellss. Finally, strong TNFR2 immunoreactivity was found on CD11b$^+$ macrophages and microglial cells, particularly in and around subpial infiltrates (Fig. 7). This study represents the first exhaustive analysis of TNF receptor expression in the mouse spinal cord, and demonstrates the presence of TNFR1 and TNFR2 on most CNS cell populations. Interestingly, both receptors are found on oligodendrocytes (although only TNFR2 appears to be in oligodendrocyte precursor cells), underscoring the critical role played by TNF signalling in oligodendrocyte function. The cell-specific expression of TNF receptors is summarized in Supplementary Table 1.

TNFR1 and TNFR2 expression profiles in the spinal cord of patients with chronic multiple sclerosis

In parallel, we analysed TNFR1 and TNFR2 expression in the post-mortem spinal cord of patients with progressive multiple sclerosis (three cases; see Supplementary Table 2). Diaminobenzidene staining for TNFR1 in the white matter, in particular at the edge of the examined chronic inactive lesions characterized by low degree of perivascular inflammatory infiltrates, showed reactivity in the cell body of cells morphologically resembling neurons (Fig. 8A). Neuronal-specific expression was confirmed with double-immunofluorescent labelling of TNFR1 with MAP2 (Fig. 8B), in agreement with our data in the mouse. Interestingly, in the same lesions, TNFR1 expression was detected surrounding CNPase$^+$ myelin rings (Fig. 8C and D), within myelin lamellas (Fig. 8C and E), and on occasional oligodendrocyte processes (Fig. 8C and F), but not on oligodendrocytes cell bodies. This suggests that TNFR1 is present in myelin-containing membrane structures wrapped around axons, and possibly on the axons as well, at the axon–oligodendrocyte interface. We can exclude that TNFR1 immunoreactivity on CNPase$^+$ myelin rings is derived from TNFR1-expressing microglia/macrophages or astrocytes in contact with the myelinated axons, since double-immunofluorescent labelling of TNFR1 with IBA1 or GFAP showed absence of TNFR1 expression on either microglia/macrophages or astrocytes (data not shown). The localization of a TNF-responsive receptor in myelin lamellas, specifically within lesions, provides strong evidence of the involvement of TNF signalling in the direct regulation of oligodendrocyte function and, perhaps, myelination. In contrast with TNFR1, TNFR2 expression was localized in activated microglia/macrophages within white matter lesions (Fig. 8G and H) and in reactive astrocytes (Fig. 8I and J). TNFR2 was not detected in neurons, and also no definitive evidence of TNFR2 expression was found in oligodendrocytes (data not shown). The cell-specific expression of TNF receptors is summarized in Supplementary Table 1.

Discussion

Our study represents a comprehensive investigation of the dual functions of soluble TNF and transmembrane TNF in the pathophysiology of EAE carried out with pharmacological inhibitors. By comparing the effects of XPro1595, a selective soluble TNF inhibitor, and etanercept, a non-selective TNF inhibitor, we directly demonstrate that transmembrane TNF signalling is necessary for functional recovery, axon preservation and, most importantly, remyelination in a murine model of multiple sclerosis. Our findings build upon genetic evidence showing that soluble TNF is acutely proinflammatory, whereas transmembrane TNF is chronically involved in repair, and suggest that pharmacological inhibition of soluble TNF may be effectively translated into a therapy for multiple sclerosis. Furthermore, this work includes a complete investigation of TNF receptor cellular localization in the spinal cord of EAE mice and of patients affected by progressive multiple sclerosis, providing a basis for a better understanding of the role of TNF signalling in the human pathology, as well as its experimental model.

The evidence emerging from our study, in addition to extensive data in the literature, leads us to formulate the hypothesis that selective blockade of soluble TNF, which has the highest affinity for TNFR1, and preservation of signalling mediated by transmembrane TNF, which conversely has the highest affinity for TNFR2, causes a shift in the balance of TNF receptor activation towards TNFR2, and the protective functions associated with transmembrane TNF would likely be attributed to TNFR2-mediated processes (Caminero *et al*., 2011). However, mindful that transmembrane TNF is also capable of activating TNFR1, we cannot exclude the possibility that transmembrane TNF-mediated TNFR1 activation could also result, at least in part, in protection.

We show that in MOG-induced EAE, inhibition of soluble TNF significantly improves the clinical outcome when administered after disease onset, hence with a clinically relevant regimen.

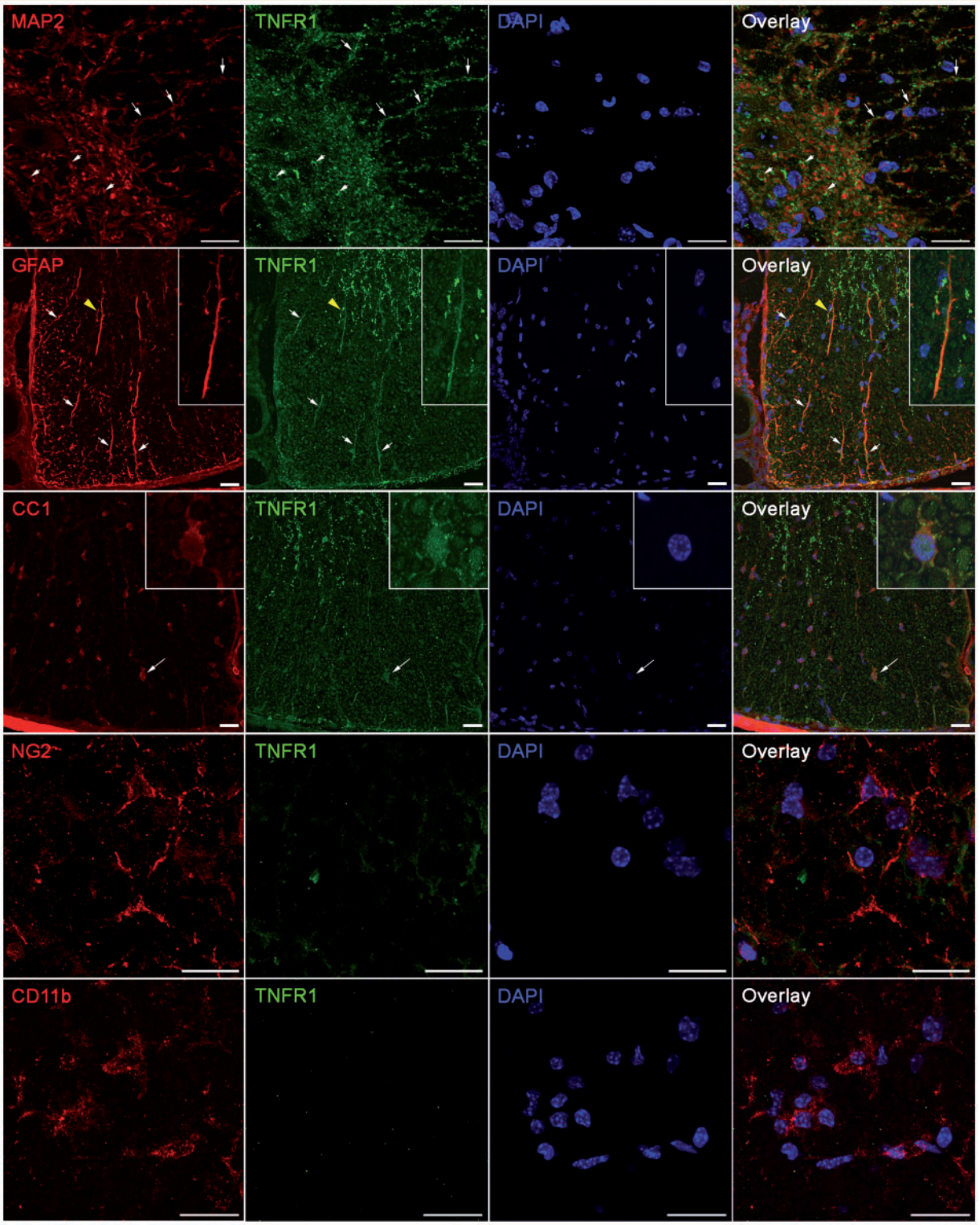

Figure 6 Characterization of TNFR1 expression and localization in the mouse spinal cord following EAE (20 days post-induction). Double-immunofluorescent labelling of TNFR1 with GFAP (astrocytes), MAP2 (neurons), CC1 (mature oligodendrocytes), NG2 (oligodendrocyte precursor cells) and CD11b (microglia/macrophages) showing TNFR1 immunoreactivity in neurons (high expression), astrocytes and mature oligodendrocytes. No expression was detected in microglia/macrophages and oligodendrocyte precursor cells. Short white arrows in all micrographs identify double-positive cells. Yellow arrowhead in GFAP micrograph and long white arrow in CC1 micrograph identify cells magnified in the corresponding insets. Scale bars = 20 μm. Images were obtained with an Olympus FluoView FV1000 confocal microscope.

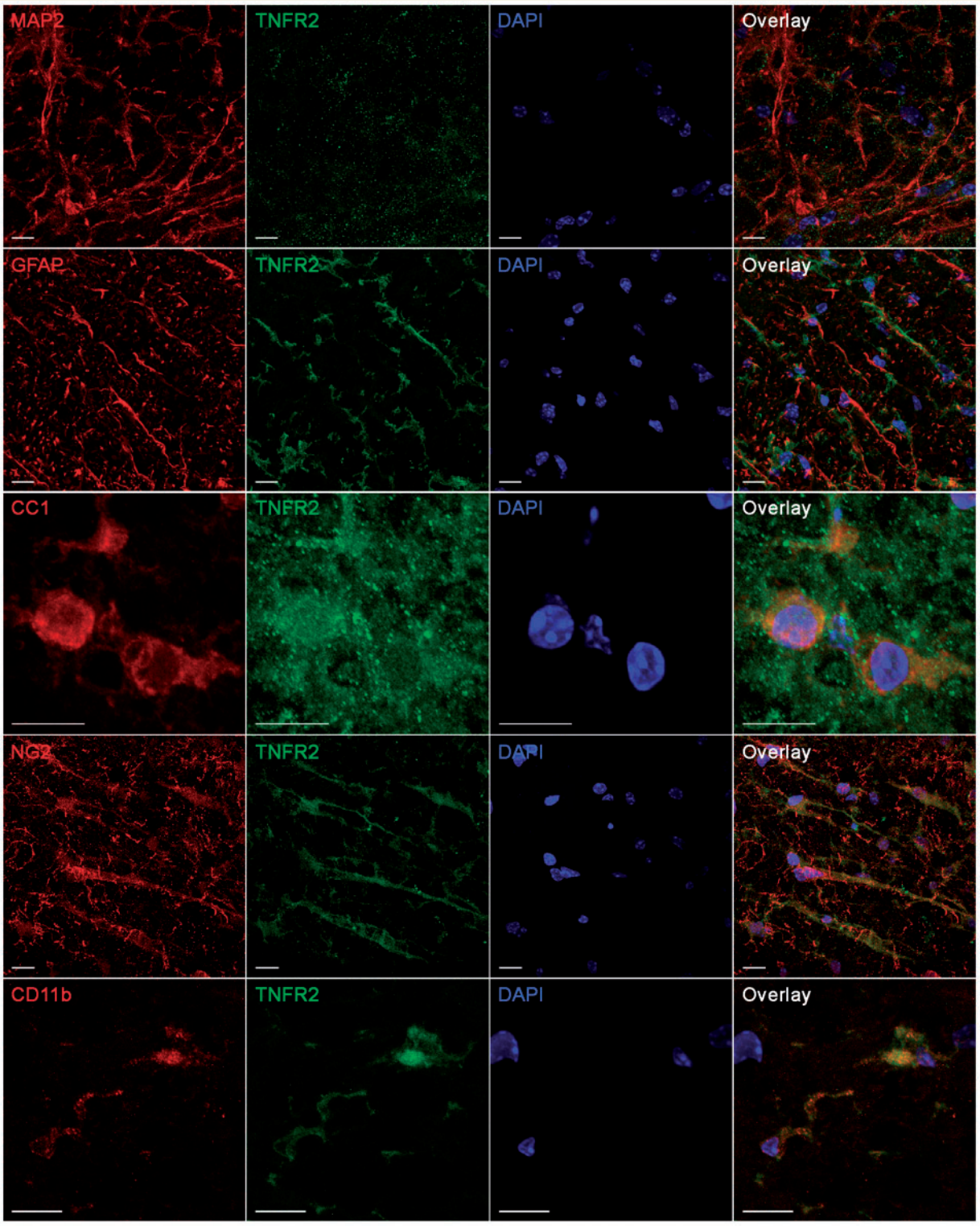

Figure 7 Characterization of TNFR2 expression and localization in the mouse spinal cord following EAE (20 days post-induction). Double-immunofluorescent labelling of TNFR2 with GFAP (astrocytes), MAP2 (neurons), CC1 (mature oligodendrocytes), NG2 (oligodendrocyte precursor cells) and CD11b (microglia/macrophages) showing TNFR2 immunoreactivity in oligodendrocytes, oligodendrocyte precursor cells, astrocytes and microglia/macrophages. No expression was found in neurons. Scale bars = 10 μm. Images were obtained with an Olympus Fluoview FV1000 confocal microscope.

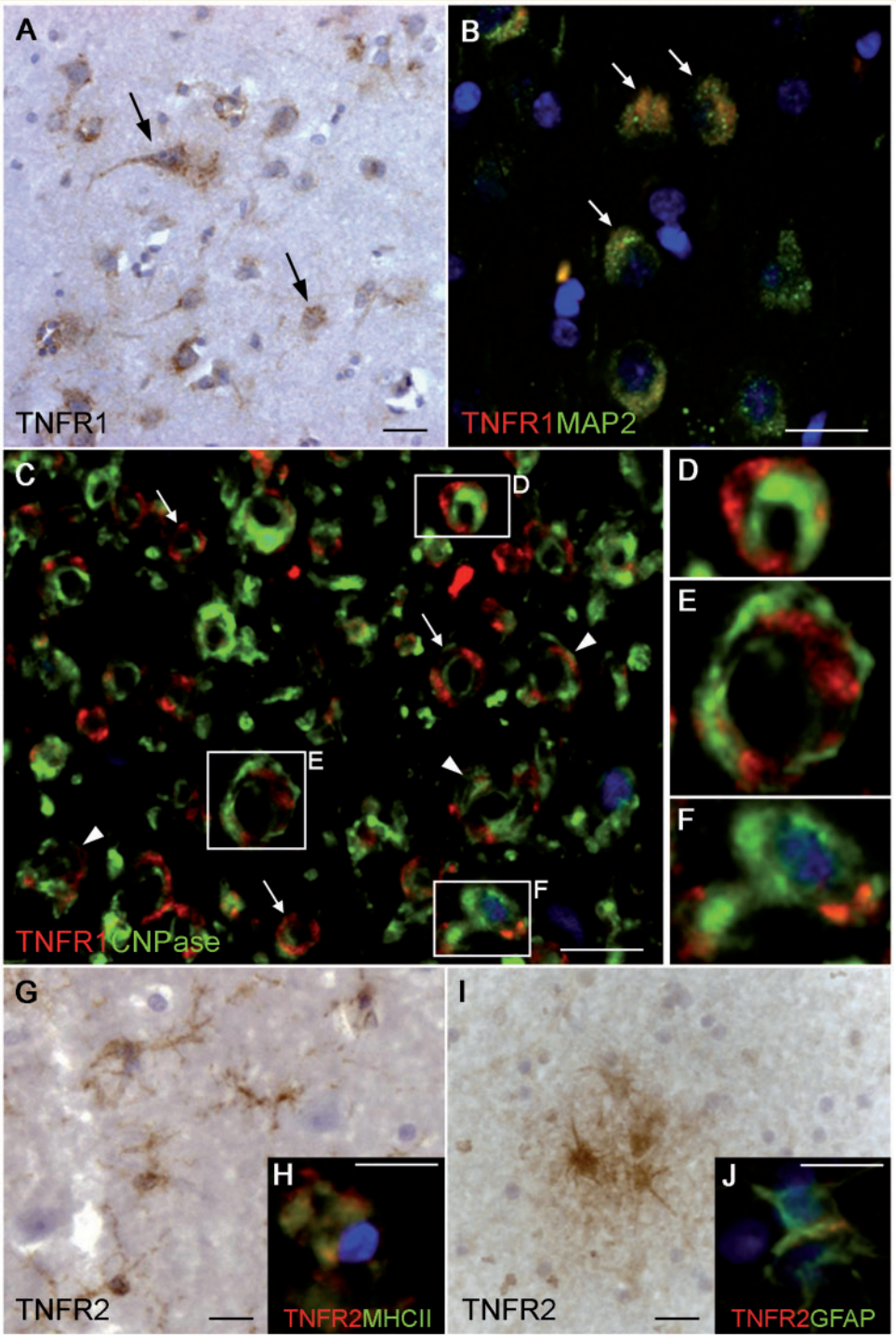

Figure 8 Characterization of TNFR expression and localization in the spinal cord of patients with progressive multiple sclerosis. (**A**) Diaminobenzidene staining of TNFR1 in the spinal cord grey matter showing TNFR1 labelling in cells morphologically resembling neurons. Black arrows point at different populations of neurons positive for TNFR1. (**B**) Double-immunofluorescent labelling of TNFR1 with MAP2, demonstrating TNFR1 expression in neurons. (**C–F**) Double-immunofluorescent labelling of TNFR1 with CNPase, showing TNFR1 expression surrounding myelin rings (white arrows in **C**; **D**), within myelin lamellas (arrowheads in **C**; **E**) and on oligodendrocyte processes (**F**) in proximity of multiple sclerosis lesions. (**G**) Diaminobenzidene staining of TNFR2 showing TNFR2 labelling in cells morphologically resembling microglia. (**H**) Double-immunofluorescent labelling of TNFR2 with MHCII, demonstrating TNFR2 expression in microglia/macrophages within lesions. (**I**) DAB staining of TNFR2 showing TNFR2 labelling in cells morphologically resembling astrocytes. (**J**) Double-immunofluorescent labelling of TNFR2 with GFAP showing TNFR2 expression in astrocytes. Scale bars = 10 μm.

After overcoming the acute phase of disease, which develops similarly to etanercept-treated and control mice, XPro1595-treated mice recover from paralysis and maintain long-term function. Although it is well documented that activation of TNFR1 signalling is associated with a proinflammatory effect that sustains the initiation phase of EAE and causes demyelination (Korner *et al.,* 1997; Akassoglou *et al*., 1998; Eugster *et al.,* 1999; Kassiotis *et al.,* 1999; Arnett *et al*., 2001; Kassiotis and Kollias, 2001; Gimenez *et al*., 2006), our data suggest that long-term improvement is not dependent, at least not exclusively, on the ability of XPro1595 to antagonize inflammation by inhibiting this pathway. Indeed, both XPro1595 and etanercept equally attenuate inflammation, as demonstrated by reduced macrophage infiltration and expression of proinflammatory cytokines and chemokines (Figs 1B and 2). Nevertheless, the anti-inflammatory effect of etanercept is not sufficient to stimulate recovery, indicating that it is the protective effect of transmembrane TNF signalling, which is unaffected by XPro1595, to ultimately drive the positive outcome in chronic disease. It is also noteworthy that, except for the reduction in macrophage infiltrates into the cord, treatment with either drug after disease onset did not alter the immune cell profile in spleen and spinal cord, particularly encephalitogenic CD4 and CD8 T cell subsets. It has been recently shown that prophylactic treatment with a TNFR1-selective antagonistic TNF mutant reduces the severity of EAE by suppressing Th1 and Th17 responses, as well as immune cell infiltration into the cord (Nomura *et al*., 2009). This is not the case in our experimental paradigm, as we begin administration after disease onset, when activation of the immune response is already underway. Based on our data, we can conclude that delayed therapeutic inhibition of soluble TNF in fully developed disease is independent of immune cell modulation, and is rather associated with a direct effect on the CNS compartment. Indeed, our findings show that XPro1595 treatment increases the number of myelinated axons and the expression of neuronal-specific molecules in EAE spinal cords, while drastically diminishing the number of degenerated axons, suggesting that transmembrane TNF may play a role in axonal sparing. Although we did not assess neuronal survival *per se*, the reduction in axonal pathology could be the consequence of the ability of transmembrane TNF to directly or indirectly activate neuroprotective cascades. Based on our hypothesis of an XPro1595-mediated balance shift towards TNFR2 activation, we can speculate that TNFR2-mediated neuroprotection is occurring, while at the same time TNFR1-mediated neurotoxic events are minimized. This concept is supported by published evidence showing that activation of TNFR2 promotes neuronal survival under a variety of pathological conditions, such as ischaemia reperfusion, glutamate- and β-amyloid-induced cytotoxicity (Shen *et al*., 1997; Fontaine *et al*., 2002; Marchetti *et al*., 2004), whereas TNFR1-mediated signalling is associated with neuronal cell death (McCoy *et al*., 2006; Wen *et al*., 2006; He *et al*., 2007; McCoy and Tansey, 2008; McAlpine *et al*., 2009). Our own immunohistochemical data show that TNFR2 is absent in neurons, both in mouse EAE and human multiple sclerosis (Figs 7 and 8), suggesting that transmembrane TNF/TNFR2-mediated neuroprotective effects occur via indirect mechanisms. On the contrary, TNFR1 is highly expressed in neurons (Figs 6 and 8); therefore, by reducing the tone of TNFR1 activation as a consequence of blocking soluble TNF, we may be directly dampening TNFR1-mediated neurotoxicity and pro-apoptotic function. This could be especially important in the human pathology, where administration of a selective soluble TNF inhibitor, by virtue of a limited neuronal TNFR1 activation, could play a role in delaying or reducing neurodegeneration, and hence prevent patient disability. On the other hand, it has also been described that NF-KB signalling engaged downstream of TNFR1 activation in neurons is responsible for counteracting TNFR1-mediated pro-apoptotic effect (Kaltschmidt *et al*., 1999; Taoufik *et al*., 2007, 2010), therefore we cannot exclude that transmembrane TNF-mediated activation of TNFR1 may be acting, at least partially, as anti-apoptotic signal preventing neuronal death. This possibility is further corroborated by the findings of Taoufik *et al*. (2011) which, in agreement with our study, demonstrate that selective inhibition of soluble TNF by XPro1595 is protective in EAE and such effect is dependent, at least in part, upon maintenance of neuroprotective neuronal NF-KB activity.

A crucial finding of our study is the demonstration that transmembrane TNF signalling is essential in preserving myelin integrity and compaction and, most importantly, in promoting remyelination. This, combined with the immunohistochemical evidence on EAE models that TNFR1 and TNFR2 are both expressed on oligodendrocytes and TNFR2 is expressed on oligodendrocyte precursor cells, suggests that TNF plays a direct role in modulating properties and functions of the oligodendrocyte compartment. In our EAE model, and in agreement with previous reports (Arnett *et al*., 2001, 2003), remyelination is accompanied by a significant increase in the number of $NG2^+$ oligodendrocyte precursor cells (Fig. 5F); therefore, a plausible scenario is that signalling mediated by transmembrane TNF via TNFR2 induces the proliferation and/or survival of oligodendrocyte precursor cells, thereby increasing the pool of cells readily available to remyelinate spared axons. We also found that oligodendrocytes express TNFR1. Hovelmeyer *et al*. (2005) have documented that TNFR1-mediated oligodendrocyte apoptosis is a key event in the induction of EAE. More recently, Paintlia *et al*. (2011) demonstrated that synergistic action of TNF and IL17 can also cause oligodendrocyte apoptosis via a TNFR1-mediated mechanism. Based on this evidence we can speculate that, by shifting the balance towards a preferential activation of TNFR2, XPro1595 may also contribute to prevent oligodendrocyte apoptosis.

Another possibility in explaining the protective effect of Xpro1595 is that transmembrane TNF is required for establishing immune tolerance. The inhibition by etanercept of transmembrane TNF signalling on specific cell populations, e.g. dendritic cells, which have tolerogenic potential (Fu and Jiang, 2010), could disrupt cross-talk with effector T cells and prevent the formation of tolerizing T cells, allowing for continued immune attack of oligodendrocyte precursor cells and oligodendrocytes resulting in ongoing demyelination.

Another important finding of our study is that TNFR2 is highly expressed in microglia following EAE (Fig. 7). It has been recently shown by Veroni *et al.* (2010) that TNFR2 stimulation in microglia promotes the expression of anti-inflammatory and neuroprotective genes such as granulocyte colony-stimulating factor (GCSF), adrenomedullin and IL-10, suggesting that microglia may contribute

to the counter-regulatory response activated in neuropathological conditions. On this basis, we can speculate that microglial TNFR2 activated by transmembrane TNF may be promoting the synthesis of protective molecules participating in the overall positive outcome of XPro1595 treatment. We also found expression of TNFR2 in microglia and macrophages localized within and around multiple sclerosis lesions in the spinal cord, suggesting that similar transmembrane TNF/TNFR2-mediated protective events could also be taking place in the human pathology. To our knowledge, this is the first report of TNFR2 expression in microglia in multiple sclerosis tissue, since thus far microglial TNFR2 was only identified in the brains of patients with AIDS (Sippy *et al*., 1995).

It should also be noted that an interesting pattern of TNFR1 expression was found in spinal cord multiple sclerosis lesions, specifically around and within $CNPase^+$ myelin rings (Fig. 3C). The presence of TNFR1 in oligodendrocyte myelin lamellas wrapped around axons, and possibly at the axon–oligodendrocyte interface, provides strong anatomical evidence of the involvement of TNF signalling in the direct regulation of oligodendrocyte function. Our finding complements previous works showing TNFR1 expression in oligodendrocytes in the brain of patients with multiple sclerosis (Raine *et al*., 1998). Similarly to the mouse, this may suggest that TNFR1 activation could lead to oligodendrocyte damage and apoptosis. Therefore, in view of a possible therapeutic application in multiple sclerosis, we can speculate that by shifting the balance towards a preferential TNFR2 activation, XPro1595 administration could result in reduction and/or inhibition of oligodendrocyte apoptosis, hence protection from demyelination.

Lastly, it is worth mentioning that, unlike etanercept, XPro1595 does not directly block lymphotoxin (Zalevsky *et al*., 2007), a cytokine belonging to the tumour necrosis factor superfamily and capable of binding to both TNFR1 and TNFR2. Lymphotoxin is secreted by activated T cells (Zipp *et al*., 1995) and is expressed in multiple sclerosis plaques (Selmaj *et al*., 1991). Although the role of lymphotoxin in EAE is controversial, most studies seem to indicate that inhibition of the lymphotoxin pathway may be protective against EAE (Aktas *et al*., 2006). Our work with XPro1595 and etanercept, although it was not specifically directed at investigating the role of lymphotoxin, seems to indicate that lymphotoxin plays a marginal role in EAE, at least in sustaining the chronic phase of the disease. Indeed XPro1595, which does not block lymphotoxin, has a chronic protective effect, while etanercept, which blocks lymphotoxin, does not show protection. We cannot exclude, however, that XPro1595 may indirectly reduce the tone of lymphotoxin signalling by reducing lymphotoxin expression, which could contribute to the protective effect of the compound in EAE.

Collectively, our data suggest that, in the balance between demyelination and remyelination, it is the positive effect of transmembrane TNF in the remyelination process that ultimately accounts for the observed functional recovery and resolution of EAE. This carries important clinical implications for multiple sclerosis therapy. Since human multiple sclerosis is primarily a relapsing–remitting disease characterized by alternating damage and repair phases, the challenge in therapies targeting multiple sclerosis is to block the damage while still allowing repair to take place. Using a pharmacological approach, here we show that soluble TNF is responsible for the damage, whereas transmembrane TNF drives the repair process. XPro1595 maintains the protective properties of TNF and allows remyelination to occur. Therefore, unlike non-selective TNF inhibitors, which are associated with demyelination when administered in human therapy, XPro1595 represents a promising new candidate to be added to the limited repertoire of multiple sclerosis modulating drugs, finally opening the door to the introduction of a TNF inhibitor into multiple sclerosis therapy.

Acknowledgements

We thank the UK MS Tissue Bank (www.ukmstissuebank.imperial.ac.uk) for providing the post-mortem multiple sclerosis samples analysed in the study. We are also grateful to Dr Mary Bunge (The Miami Project To Cure Paralysis, University of Miami Miller School of Medicine) for her invaluable advice on morphological evaluation and interpretation of EM micrographs. The authors do not have any conflicting financial interests. It should be noted, however, that D.E.S. is an employee of Xencor, which provided the compound XPro1595 used in the study.

Funding

National Institutes of Health (NS051709, NS065479 to J.R.B.); The Miami Project To Cure Paralysis.

Supplementary material

Supplementary material is available at *Brain* online.

References

Akassoglou K, Bauer J, Kassiotis G, Pasparakis M, Lassmann H, Kollias G, et al. Oligodendrocyte apoptosis and primary demyelination induced by local TNF/p55TNF receptor signaling in the central nervous system of transgenic mice: models for multiple sclerosis with primary oligodendrogliopathy. Am J Pathol 1998; 153: 801–13.

Aktas O, Prozorovski T, Zipp F. Death ligands and autoimmune demyelination. Neuroscientist 2006; 12: 305–16.

Alexopoulou L, Kranidioti K, Xanthoulea S, Denis M, Kotanidou A, Douni E, et al. Transmembrane TNF protects mutant mice against intracellular bacterial infections, chronic inflammation and autoimmunity. Eur J Immunol 2006; 36: 2768–80.

Arnett HA, Mason J, Marino M, Suzuki K, Matsushima GK, Ting JP. TNF alpha promotes proliferation of oligodendrocyte progenitors and remyelination. Nat Neurosci 2001; 4: 1116–22.

Arnett HA, Wang Y, Matsushima GK, Suzuki K, Ting JP. Functional genomic analysis of remyelination reveals importance of inflammation in oligodendrocyte regeneration. J Neurosci 2003; 23: 9824–32.

Baker D, Butler D, Scallon BJ, O'Neill JK, Turk JL, Feldmann M. Control of established experimental allergic encephalomyelitis by inhibition of tumor necrosis factor (TNF) activity within the central nervous system using monoclonal antibodies and TNF receptor-immunoglobulin fusion proteins. Eur J Immunol 1994; 24: 2040–8.

Brambilla R, Persaud T, Hu X, Karmally S, Shestopalov VI, Dvoriantchikova G, et al. Transgenic inhibition of astroglial NF-kappa B improves functional outcome in experimental autoimmune

encephalomyelitis by suppressing chronic central nervous system inflammation. J Immunol 2009; 182: 2628–40.
Caminero A, Comabella M, Montalban X. Tumor necrosis factor alpha (TNF-alpha), anti-TNF-alpha and demyelination revisited: An ongoing story. J Neuroimmunol 2011; 234: 1–6.
Canault M, Peiretti F, Mueller C, Kopp F, Morange P, Rihs S, et al. Exclusive expression of transmembrane TNF-alpha in mice reduces the inflammatory response in early lipid lesions of aortic sinus. Atherosclerosis 2004; 172: 211–8.
Dal Canto RA, Shaw MK, Nolan GP, Steinman L, Fathman CG. Local delivery of TNF by retrovirus-transduced T lymphocytes exacerbates experimental autoimmune encephalomyelitis. Clin Immunol 1999; 90: 10–4.
Eugster HP, Frei K, Bachmann R, Bluethmann H, Lassmann H, Fontana A. Severity of symptoms and demyelination in MOG-induced EAE depends on TNFR1. Eur J Immunol 1999; 29: 626–32.
Fontaine V, Mohand-Said S, Hanoteau N, Fuchs C, Pfizenmaier K, Eisel U. Neurodegenerative and neuroprotective effects of tumor Necrosis factor (TNF) in retinal ischemia: opposite roles of TNF receptor 1 and TNF receptor 2. J Neurosci 2002; 22: RC216.
Fromont A, De Seze J, Fleury MC, Maillefert JF, Moreau T. Inflammatory demyelinating events following treatment with anti-tumor necrosis factor. Cytokine 2009; 45: 55–7.
Fu C, Jiang A. Generation of tolerogenic dendritic cells via the E-cadherin/beta-catenin-signaling pathway. Immunol Res 2010; 46: 72–8.
Gimenez MA, Sim J, Archambault AS, Klein RS, Russell JH. A tumor necrosis factor receptor 1-dependent conversation between central nervous system-specific T cells and the central nervous system is required for inflammatory infiltration of the spinal cord. Am J Pathol 2006; 168: 1200–9.
Goffe B, Cather JC. Etanercept: an overview. J Am Acad Dermatol 2003; 49: S105–11.
Grell M, Douni E, Wajant H, Lohden M, Clauss M, Maxeiner B, et al. The transmembrane form of tumor necrosis factor is the prime activating ligand of the 80 kDa tumor necrosis factor receptor. Cell 1995; 83: 793–802.
He P, Zhong Z, Lindholm K, Berning L, Lee W, Lemere C, et al. Deletion of tumor necrosis factor death receptor inhibits amyloid beta generation and prevents learning and memory deficits in Alzheimer's mice. J Cell Biol 2007; 178: 829–41.
Hofman FM, Hinton DR, Johnson K, Merrill JE. Tumor necrosis factor identified in multiple sclerosis brain. J Exp Med 1989; 170: 607–12.
Holtmann MH, Neurath MF. Differential TNF-signaling in chronic inflammatory disorders. Curr Mol Med 2004; 4: 439–44.
Hovelmeyer N, Hao Z, Kranidioti K, Kassiotis G, Buch T, Frommer F, et al. Apoptosis of oligodendrocytes via Fas and TNF-R1 is a key event in the induction of experimental autoimmune encephalomyelitis. J Immunol 2005; 175: 5875–84.
Ierna MX, Scales HE, Mueller C, Lawrence CE. Transmembrane tumor necrosis factor alpha is required for enteropathy and is sufficient to promote parasite expulsion in gastrointestinal helminth infection. Infect Immun 2009; 77: 3879–85.
Kaltschmidt B, Uherek M, Wellmann H, Volk B, Kaltschmidt C. Inhibition of NF-kappaB potentiates amyloid beta-mediated neuronal apoptosis. Proc Natl Acad Sci USA 1999; 96: 9409–14.
Kassiotis G, Kollias G. Uncoupling the proinflammatory from the immunosuppressive properties of tumor necrosis factor (TNF) at the p55 TNF receptor level: implications for pathogenesis and therapy of autoimmune demyelination. J Exp Med 2001; 193: 427–34.
Kassiotis G, Pasparakis M, Kollias G, Probert L. TNF accelerates the onset but does not alter the incidence and severity of myelin basic protein-induced experimental autoimmune encephalomyelitis. Eur J Immunol 1999; 29: 774–80.
Korner H, Riminton DS, Strickland DH, Lemckert FA, Pollard JD, Sedgwick JD. Critical points of tumor necrosis factor action in central nervous system autoimmune inflammation defined by gene targeting. J Exp Med 1997; 186: 1585–90.
Lenercept-Group. TNF neutralization in MS: results of a randomized, placebo-controlled multicenter study. The Lenercept Multiple Sclerosis Study Group and The University of British Columbia MS/MRI Analysis Group. Neurology 1999; 53: 457–65.
Liu J, Marino MW, Wong G, Grail D, Dunn A, Bettadapura J, et al. TNF is a potent anti-inflammatory cytokine in autoimmune-mediated demyelination. Nat Med 1998; 4: 78–83.
Maimone D, Gregory S, Arnason BG, Reder AT. Cytokine levels in the cerebrospinal fluid and serum of patients with multiple sclerosis. J Neuroimmunol 1991; 32: 67–74.
Marchetti L, Klein M, Schlett K, Pfizenmaier K, Eisel UL. Tumor necrosis factor (TNF)-mediated neuroprotection against glutamate-induced excitotoxicity is enhanced by N-methyl-D-aspartate receptor activation. Essential role of a TNF receptor 2-mediated phosphatidylinositol 3-kinase-dependent NF-kappa B pathway. J Biol Chem 2004; 279: 32869–81.
McAlpine FE, Lee JK, Harms AS, Ruhn KA, Blurton-Jones M, Hong J, et al. Inhibition of soluble TNF signaling in a mouse model of Alzheimer's disease prevents pre-plaque amyloid-associated neuropathology. Neurobiol Dis 2009; 34: 163–77.
McCoy MK, Martinez TN, Ruhn KA, Szymkowski DE, Smith CG, Botterman BR, et al. Blocking soluble tumor necrosis factor signaling with dominant-negative tumor necrosis factor inhibitor attenuates loss of dopaminergic neurons in models of Parkinson's disease. J Neurosci 2006; 26: 9365–75.
McCoy MK, Tansey MG. TNF signaling inhibition in the CNS: implications for normal brain function and neurodegenerative disease. J Neuroinflammation 2008; 5: 45.
Nomura T, Abe Y, Kamada H, Shibata H, Kayamuro H, Inoue M, et al. Therapeutic effect of PEGylated TNFR1-selective antagonistic mutant TNF in experimental autoimmune encephalomyelitis mice. J Control Release 2011; 149: 8–14.
Olleros ML, Guler R, Vesin D, Parapanov R, Marchal G, Martinez-Soria E, et al. Contribution of transmembrane tumor necrosis factor to host defense against Mycobacterium bovis bacillus Calmette-guerin and Mycobacterium tuberculosis infections. Am J Pathol 2005; 166: 1109–20.
Olleros ML, Vesin D, Lambou AF, Janssens JP, Ryffel B, Rose S, et al. Dominant-negative tumor necrosis factor protects from Mycobacterium bovis Bacillus Calmette Guerin (BCG) and endotoxin-induced liver injury without compromising host immunity to BCG and Mycobacterium tuberculosis. J Infect Dis 2009; 199: 1053–63.
Paintlia MK, Paintlia AS, Singh AK, Singh I. Synergistic activity of interleukin-17 and tumor necrosis factor-alpha enhances oxidative stress-mediated oligodendrocyte apoptosis. J Neurochem 2011; 116: 508–21.
Pasparakis M, Alexopoulou L, Episkopou V, Kollias G. Immune and inflammatory responses in TNF alpha-deficient mice: a critical requirement for TNF alpha in the formation of primary B cell follicles, follicular dendritic cell networks and germinal centers, and in the maturation of the humoral immune response. J Exp Med 1996; 184: 1397–411.
Probert L, Akassoglou K, Pasparakis M, Kontogeorgos G, Kollias G. Spontaneous inflammatory demyelinating disease in transgenic mice showing central nervous system-specific expression of tumor necrosis factor alpha. Proc Natl Acad Sci USA 1995; 92: 11294–8.
Raine CS, Bonetti B, Cannella B. Multiple sclerosis: expression of molecules of the tumor necrosis factor ligand and receptor families in relationship to the demyelinated plaque. Rev Neurol 1998; 154: 577–85.
Ramos-Casals M, Brito-Zeron P, Soto MJ, Cuadrado MJ, Khamashta MA. Autoimmune diseases induced by TNF-targeted therapies. Best Pract Res Clin Rheumatol 2008; 22: 847–61.
Ruddle NH, Bergman CM, McGrath KM, Lingenheld EG, Grunnet ML, Padula SJ, et al. An antibody to lymphotoxin and tumor necrosis factor

prevents transfer of experimental allergic encephalomyelitis. J Exp Med 1990; 172: 1193–200.

Selmaj K, Raine CS, Cannella B, Brosnan CF. Identification of lymphotoxin and tumor necrosis factor in multiple sclerosis lesions. J Clin Invest 1991; 87: 949–54.

Sfikakis PP. The first decade of biologic TNF antagonists in clinical practice: lessons learned, unresolved issues and future directions. Curr Dir Autoimmun 2010; 11: 180–210.

Sharief MK, Hentges R. Association between tumor necrosis factor-alpha and disease progression in patients with multiple sclerosis. N Engl J Med 1991; 325: 467–72.

Shen Y, Li R, Shiosaki K. Inhibition of p75 tumor necrosis factor receptor by antisense oligonucleotides increases hypoxic injury and beta-amyloid toxicity in human neuronal cell line. J Biol Chem 1997; 272: 3550–3.

Sippy BD, Hofman FM, Wallach D, Hinton DR. Increased expression of tumor necrosis factor-alpha receptors in the brains of patients with AIDS. J Acquir Immune Defic Syndr Hum Retrovirol 1995; 10: 511–21.

Spuler S, Yousry T, Scheller A, Voltz R, Holler E, Hartmann M, et al. Multiple sclerosis: prospective analysis of TNF-alpha and 55 kDa TNF receptor in CSF and serum in correlation with clinical and MRI activity. J Neuroimmunol 1996; 66: 57–64.

Steed PM, Tansey MG, Zalevsky J, Zhukovsky EA, Desjarlais JR, Szymkowski DE, et al. Inactivation of TNF signaling by rationally designed dominant-negative TNF variants. Science 2003; 301: 1895–8.

Suvannavejh GC, Lee HO, Padilla J, Dal Canto MC, Barrett TA, Miller SD. Divergent roles for p55 and p75 tumor necrosis factor receptors in the pathogenesis of MOG(35-55)-induced experimental autoimmune encephalomyelitis. Cell Immunol 2000; 205: 24–33.

Szalai AJ, Nataf S, Hu XZ, Barnum SR. Experimental allergic encephalomyelitis is inhibited in transgenic mice expressing human C-reactive protein. J Immunol 2002; 168: 5792–7.

Taoufik E, Petit E, Divoux D, Tseveleki V, Mengozzi M, Roberts ML, et al. TNF receptor I sensitizes neurons to erythropoietin- and VEGF-mediated neuroprotection after ischemic and excitotoxic injury. Proc Natl Acad Sci USA 2010; 105: 6185–90.

Taoufik E, Valable S, Muller GJ, Roberts ML, Divoux D, Tinel A, et al. FLIP(L) protects neurons against in vivo ischemia and in vitro glucose deprivation-induced cell death. J Neurosci 2007; 27: 6633–46.

Taoufik D, et al. 2011.

Tracey D, Klareskog L, Sasso EH, Salfeld JG, Tak PP. Tumor necrosis factor antagonist mechanisms of action: a comprehensive review. Pharmacol Ther 2008; 117: 244–79.

Trapp BD, Peterson J, Ransohoff RM, Rudick R, Mork S, Bo L. Axonal transection in the lesions of multiple sclerosis. N Engl J Med 1998; 338: 278–85.

van Loo G, De Lorenzi R, Schmidt H, Huth M, Mildner A, Schmidt-Supprian M, et al. Inhibition of transcription factor NF-kappaB in the central nervous system ameliorates autoimmune encephalomyelitis in mice. Nat Immunol 2006; 7: 954–61.

Veroni C, Gabriele L, Canini I, Castiello L, Coccia E, Remoli ME, et al. Activation of TNF receptor 2 in microglia promotes induction of anti-inflammatory pathways. Mol Cell Neurosci 2010; 45: 234–44.

Wajant H, Pfizenmaier K, Scheurich P. Tumor necrosis factor signaling. Cell Death Differ 2003; 10: 45–65.

Wallis RS. Infectious complications of tumor necrosis factor blockade. Curr Opin Infect Dis 2009; 22: 403–9.

Wen W, Sanelli T, Ge W, Strong W, Strong MJ. Activated microglial supernatant induced motor neuron cytotoxicity is associated with upregulation of the TNFR1 receptor. Neurosci Res 2006; 55: 87–95.

Zalevsky J, Secher T, Ezhevsky SA, Janot L, Steed PM, O'Brien C, et al. Dominant-negative inhibitors of soluble TNF attenuate experimental arthritis without suppressing innate immunity to infection. J Immunol 2007; 179: 1872–83.

Zipp F, Weber F, Huber S, Sotgiu S, Czlonkowska A, Holler E, et al. Genetic control of multiple sclerosis: increased production of lymphotoxin and tumor necrosis factor-alpha by HLA-DR2 + T cells. Ann Neurol 1995; 38: 723–30.